Transition from single-mode to multimode operation of an injection-seeded pulsed optical parametric oscillator

Richard T. White, Yabai He, and Brian J. Orr

Centre for Lasers and Applications, Macquarie University, Sydney, 2109, Australia

Mitsuhiko Kono and K. G. H. Baldwin

Research School of Physical Sciences & Engineering, Australian National University, Canberra, 0200, Australia
Kenneth.Baldwin@anu.edu.au

Abstract: Optical-heterodyne measurements are made on ~842-nm signal output of an injection-seeded optical parametric oscillator (OPO) based on periodically poled $KTiOPO_4$ pumped at 532 nm by long (~27-ns) pulses from a Nd:YAG laser. At low pump energies ($\leq$ 2.5 times the free-running threshold), the narrowband tunable OPO output is single-longitudinal-mode (SLM) and frequency chirp can be <10 MHz, much less than the transform-limited optical bandwidth (~17.5 MHz). We explore the transition from SLM operation to multimode operation as pump energy or phase mismatch are increased, causing unseeded cavity modes to build up later in the pulse.

OCIS codes: (120.5050) Phase measurement; (190.4970) Parametric oscillators and amplifiers

References and Links

1. R. T. White, Y. He, B. J. Orr, M. Kono, and K. G. H. Baldwin, "Control of frequency chirp in nanosecond-pulsed laser spectroscopy. 2. A long-pulse optical parametric oscillator for narrow optical bandwidth," J. Opt. Soc. Am. B, **21**, 1586-1594 (2004).
2. R. T. White, Y. He, B. J. Orr, M. Kono, and K. G. H. Baldwin, "Pulsed injection-seeded optical parametric oscillator with low frequency chirp for high-resolution spectroscopy," Opt. Lett. **28**, 1248-1250 (2003).
3. R. T. White, Y. He, B. J. Orr, M. Kono, and K. G. H. Baldwin, "Control of frequency chirp in nanosecond-pulsed laser spectroscopy. 1. Optical-heterodyne chirp analysis techniques," J. Opt. Soc. Am. B, **21**, 1577-1585 (2004).
4. M.S. Fee, K. Danzmann, and S. Chu, "Optical heterodyne measurement of pulsed lasers: Toward high-precision pulsed spectroscopy," Phys. Rev. A **45**, 4911-4924 (1992).
5. S. Gangopadhyay, N. Melikechi, and E. E. Eyler, "Optical phase perturbations in nanosecond pulsed amplification and second-harmonic generation," J. Opt. Soc. Am. B **11**, 231-241 (1994).
6. N. Melikechi, S. Gangopadhyay, and E. E. Eyler, "Phase dynamics in nanosecond pulsed dye laser amplification," J. Opt. Soc. Am. B **11**, 2402-2411 (1994).
7. S. D. Bergeson, K. G. H. Baldwin, T. B. Lucatorto, T. J. McIlrath, C. H. Cheng, and E. E. Eyler, "Doppler-free two-photon spectroscopy in the vacuum ultraviolet: helium $1\,^1S - 2\,^1S$ transition," J. Opt. Soc. Am. B **17**, 1599-1606 (2000).
8. J. E. Bjorkholm and H. G. Danielmeyer, "Frequency control of a pulsed nanosecond optical parametric oscillators by radiation injection," Appl. Phys. Lett. **15**, 171-173 (1969).
9. A. Fix and R. Wallenstein, "Spectral properties of pulsed nanosecond optical parametric oscillators: experimental investigations and numerical analysis," J. Opt. Soc. Am. B **13**, 2484-2497 (1996).
10. A. V. Smith, W. J. Alford, T. D. Raymond, and M. S. Bowers, "Comparison of a numerical model with measured performance of a seeded, nanosecond KTP optical parametric oscillator," J. Opt. Soc. Am. B **12**, 2253 - 2267 (1995).
11. P. Mahnke and H. H. Klingenberg, "Observation and analysis of mode competition in optic parametric oscillators," Appl. Phys. B **78**, 171-177 (2004).
12. Y. He, G. W. Baxter, and B. J. Orr, "Locking the cavity of a pulsed periodically poled lithium niobate optical parametric oscillator to the wavelength of a continuous-wave injection seeder by an 'intensity-dip' method," Rev. Sci. Instrum. **70**, 3203-3213 (1999).
13. Y. He and B. J. Orr, "Tunable single-mode operation of a pulsed optical parametric oscillator pumped by a multimode laser," Appl. Opt. **40**, 4836-4848 (2001).

#5338 - $15.00 US Received 20 September 2004; revised 3 November 2004; accepted 4 November 2004

1. Introduction

We recently reported a high-performance optical parametric oscillator (OPO) system suitable for advanced high-resolution spectroscopic applications [1]. It generates single-longitudinal-mode (SLM) pulsed coherent signal and idler output radiation that is continuously tunable with narrow optical bandwidth (<20 MHz) and low frequency chirp (<10 MHz). Its nonlinear-optical medium is periodically poled $KTiOPO_4$ (PPKTP), pumped at 532 nm by the second harmonic of a SLM Nd:YAG laser and injection-seeded at a signal wavelength λ_s of ~842 nm. The Nd:YAG pump radiation used in this work has a relatively long full-width-at-half-maximum (FWHM) pulse duration of ~27 ns (3.5 times that used in an 8-ns pulsed OPO system [2]), thereby reducing the Fourier-transform (FT) limit of the resulting OPO output pulses (~25-ns FWHM) to ~17.5 MHz FWHM.

Optical phase properties of coherent radiation from this OPO can be measured by optical heterodyne (OH) techniques [1–3], in which pulsed OPO radiation beats against cw radiation that is generated by using an acousto-optic modulator (AOM) to frequency-shift output from the cw tunable diode laser (TDL) that simultaneously injection-seeds the OPO. Three distinct OH-based approaches to chirp analysis have previously been evaluated, namely, FT, direct fit, and electronic mixer techniques [3]. The FT approach to chirp analysis, as portrayed in Fig. 1, is widely used [3–7]; we apply it here to study dynamics of the transition from SLM operation to partially seeded, multimode operation within the ~25-ns duration of the OPO pulse.

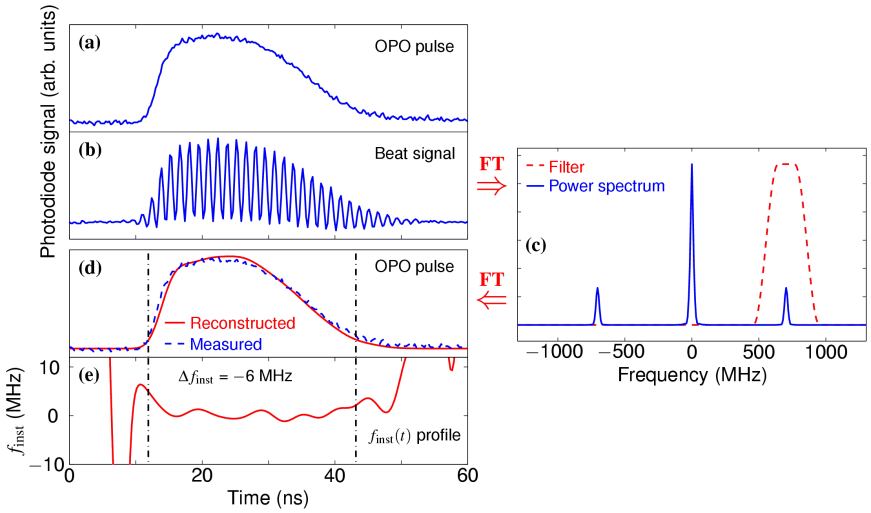

Fig. 1. Example of the FT chirp analysis procedure for output from a long-pulse injection-seeded PPKTP OPO. Traces (a) and (b) depict the measured temporal profiles for amplitude and OH beat waveform, respectively, as measured for an actual OPO signal pulse. The FT algorithm converts trace (b) into the power spectrum in trace (c), where two OH sidebands are displaced from a central peak by the AOM frequency (~730 MHz), then one OH sideband is electronically filtered and FT-analysed to yield the temporal profiles of reconstructed OPO pulse amplitude and instantaneous frequency $f_{inst}(t)$ in traces (d) and (e), respectively. Vertical dashed lines indicate 10%-intensity points of the OPO pulses, indicating the range over which frequency chirp can be (conservatively) estimated. The pump-pulse energy (64 μJ) is twice the unseeded threshold level and the PPKTP temperature is T_{PPKTP} = 125.0°C, so that the signal wavelength of the free-running PPKTP OPO is λ_{free} = 841.75 ± 0.02 nm. The TDL-seeded signal wavelength λ_s (841.76 ± 0.01 nm) is virtually identical to λ_{free}; this minimizes phase mismatch and attains a frequency chirp of less than 10 MHz, as seen in the f_{inst} profile in trace (e). (104 KB movie of a dynamic sequence of temporal profiles for 20 successive OPO pulses.)

Since the first report of an injection-seeded pulsed OPO [8], it has been clear that single-frequency operation requires the pump-pulse energy to be depleted by oscillation on one longitudinal mode of the OPO cavity (i.e., the seeded mode) well before other modes start to oscillate. It is understood that an injection-seeded OPO pulse cannot be maintained at a single

#5338 - $15.00 US Received 20 September 2004; revised 3 November 2004; accepted 4 November 2004

frequency indefinitely, as unseeded modes eventually build up from noise in the nonlinear-optical medium later in the pump pulse. It is not practical (even with a very short cavity [9]) to discriminate against other modes by having the longitudinal-mode spacing exceed the optical bandwidth of the free-running (unseeded) OPO.

Our own early measurements and modeling of the onset of broadband unseeded operation of birefringently phase-matched β-BaB_2O_4 (BBO) OPOs have been surveyed elsewhere [1]. Other experiments [9] on a short-cavity BBO OPO have revealed the statistical build-up of multimode pulsed OPO output with and without injection seeding. Likewise, spatial and temporal characteristics of a pulsed, seeded KTP OPO have been investigated in detail [10], while mode-competition effects in a KTP OPO, simultaneously seeded by two SLM TDL sources, have recently been examined [11]. Until now, a direct, clear dynamical view of the transition from SLM to multimode operation of a pulsed OPO has proved elusive.

2. Methodology and instrumentation

A representative set of temporal and frequency profiles, extracted from observed output of the long-pulse OPO, is shown in Fig. 1. The successive FT analysis steps [3] needed to process such measurements are indicated by arrows. The FT algorithm enables us to process the beat waveform in trace (b) and to extract from it the temporal profiles of the narrowband OPO pulse amplitude [reconstructed in trace (d)] for comparison with measured amplitude profiles [trace (a)], and to extract the resulting instantaneous frequency $f_{inst}(t)$ [trace (e)]. A key step [trace (c)] entails isolating one of the two OH sidebands (each displaced from the central peak in the power spectrum by the AOM frequency of ~730 MHz) using a Tukey filter (~400 MHz FWHM) [1,3] prior to the second FT step. Narrowband signal output pulse characteristics as in Fig. 1 are reproducible from pulse to pulse [1]. Click here to view a dynamic sequence of time profiles, as in Figs 1(a,b,d,e). Their mean unsigned overall chirp value $\langle|\Delta f_{inst}|\rangle$ is 13 ± 4 MHz (or 7 ± 2 MHz with more realistic 50%-intensity limits [1,2]); absolute-frequency scatter (±18 MHz) for these pulses is not shown. The instrument layout is shown in Fig. 2.

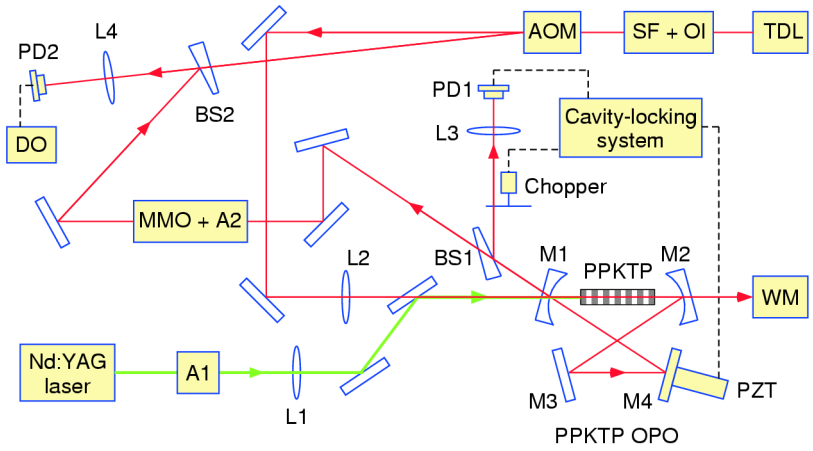

Fig. 2. Schematic of the long-pulse injection-seeded PPKTP OPO and its OH detection system. A1, A2: attenuators. AOM: acousto-optic modulator (~730 MHz). BS1, BS2: beam splitters. DO: digital oscilloscope. L1 – L4: lenses. M1 – M4: cavity mirrors. MMO: mode-matching optics. OI: optical isolator. PD1, PD2: fast photodetectors. PZT: piezoelectric translator. SF: spatial filter. TDL: tunable diode laser. WM: pulsed wavemeter.

Details of the PPKTP OPO and the OH detection system used to measure instantaneous-frequency characteristics of its signal output have been described elsewhere [1–3]. Essential features of the instrument shown in Fig. 2 are as follows: a high-performance, long-pulse SLM Nd:YAG pump laser; a four-mirror OPO ring cavity containing a temperature-controlled PPKTP crystal; a TDL injection seeder delivering continuously tunable cw SLM radiation (~5 mW at ~842 nm) *via* an optical isolator and spatial filter; a piezoelectrically

#5338 - $15.00 US Received 20 September 2004; revised 3 November 2004; accepted 4 November 2004

controlled "intensity-dip" cavity locking system [1,2,12,13] that maintains the OPO cavity in resonance at a signal wavelength λ_s coincident with that of the TDL injection seeder; an AOM driven at ~730 MHz, with the undiffracted seed beam directed into the OPO cavity while the diffracted, frequency-shifted beam is combined with output from the OPO system to generate OH beats on a 1-GHz square-law photodetector [1–3]. Additional optical parametric amplifier (OPA) stages can be added for higher-power applications. A pulsed wavemeter (Burleigh 4500-1) was used for wavelength measurement. We noticed that the wavemeter reading depends slightly on alignment and spectral bandwidth of the input beam.

Figure 3 shows pictorial aspects of the pulsed tunable OPO and OH detection system and its performance, including the quasi-Gaussian beam profiles obtained from the SLM PPKTP OPO. The long-pulse SLM Nd:YAG pump laser is at the left-hand edge of the group picture.

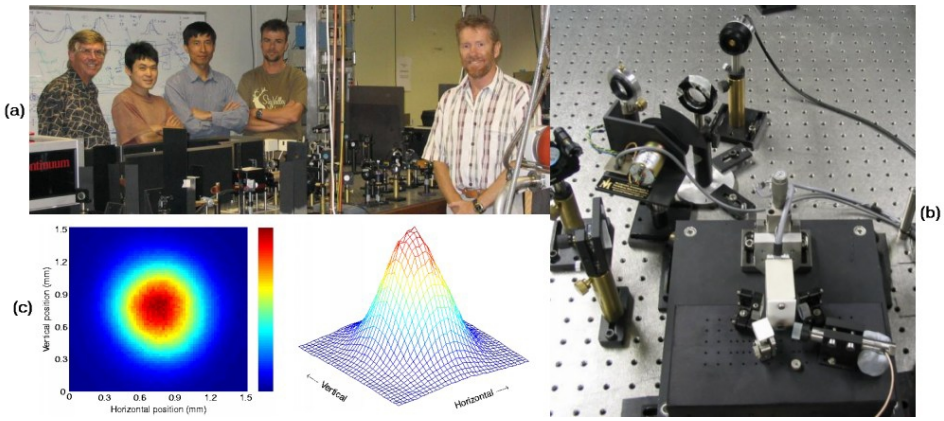

Fig. 3. (a) The authors (from left: BJO, MK, YH, RTW, and KGHB) with the pulsed tunable OPO and OH detection system. (b) The four-mirror ring cavity of the injection-seeded PPKTP OPO and its cavity-locking feedback system. (c) False-color images of the transverse profile of the SLM signal output beam from the PPKTP OPO, measured at a distance of 20 cm from the beam waist (for which w_0 = 110 μm) by a Spiricon LBA-100A and Pulnix TM-745 system.

3. Transition from SLM to multimode operation

An injection-seeded OPO cannot sustain SLM operation indefinitely because free-running oscillation on other (unseeded) modes eventually builds up from noise. Such multimode operation typically occurs earlier in an OPO pulse if the pump-laser energy is increased and its onset is aggravated if the seed wavelength is not centered on the peak of the spectral gain profile for the free-running OPO. It is possible to sustain SLM operation in many injection-seeded OPOs with short pulse durations (< 10 ns), such as those based on quasi-phase-matched nonlinear-optical materials such as PPKTP [2,3] and periodically poled $LiNbO_3$ (PPLN) [12,13]. Reliable SLM operation is feasible throughout each pulse because the build-up time for free-running modes exceeds the pump-pulse duration; this is particularly true of OPOs with optical damage thresholds that limit the allowable maximum pump-pulse energy.

The build-up of multimode operation becomes a significant problem in OPOs when longer pump-pulse durations (e.g., ~27 ns [1]) are used to produce a narrower FT-limited optical bandwidth. In recent OH measurements [1], irregularities were observed in temporal profiles of the long-pulse PPKTP OPO signal output at higher pump-laser energy (~3 times unseeded OPO threshold) and at a large value of $(\lambda_s - \lambda_{free}) \approx 0.2$ nm. It was recognized [1] that such irregularities provided a dynamic, time-resolved view of the above-mentioned transition from SLM to multimode OPO operation. We now consolidate those preliminary observations with a more systematic study of such transient effects, taking advantage of our OH techniques and the FT algorithm [1–3] together with our long-pulse SLM PPKTP OPO system [1,3].

Figure 4 shows two sets of temporal profiles for PPKTP OPO signal output with T_{PPKTP} = 125.6°C, comprising: measured beat waveforms (a,d); measured OPO signal-pulse amplitude

#5338 - $15.00 US Received 20 September 2004; revised 3 November 2004; accepted 4 November 2004

in the dashed curves of traces (b,e); reconstructed narrowband components of the OPO signal-pulse amplitude in the solid curves of traces (b,e); instantaneous-frequency chirp profiles (c,f). For these measurements, $\lambda_s \approx \lambda_{free} = 841.78$ nm. In the left-hand part of Fig. 4, the OPO pump-pulse energy is low (21 μJ), so that its ratio to unseeded PPKTP OPO threshold (13.5 μJ in this set of measurements) is $R_p = 1.55$; the right-hand part of Fig. 4 is obtained with a much higher OPO pump-pulse energy, 47 μJ ($R_p = 3.5$). Traces (a)–(c) are similar in some respects to traces (a), (b), (d), and (e) of Fig. 1 (where $R_p = 2.0$). The corresponding frequency chirp measured with $R_p < 3.0$ in this set of experiments is –16 ± 5 MHz, consistent with previous chirp measurements at small phase mismatch [1]. Traces (d)–(f) of Fig. 4 show the final stage ($R_p = 3.5$) of a series of FT-analysed OH measurements with the OPO pump-pulse energy (and hence the times-above-threshold ratio R_p) varied in the regime where partially seeded multimode operation takes over from SLM operation. Irregularities in all four forms of temporal profile appear at a transition point ~18 ns after the start of the OPO signal output pulse, which has a duration of ~25 ns FWHM. These are evident in the substantial difference between the measured (dashed) and reconstructed (solid) OPO signal-pulse intensity profiles in Fig. 4(e); the former increases markedly at the build-up of partially seeded multimode operation (because more than one OPO cavity mode is now oscillating), whereas the latter drops dramatically at the same transition point (because the FT algorithm extracts only the narrowband portion of the OPO signal-pulse amplitude). Such comparisons provide a dynamic measure of the spectral purity of the coherent light pulse as it evolves in time. Corresponding results recorded (but not shown explicitly in Fig. 4) with $R_p = 3.0$ exhibit a similar, although much less pronounced, transition point at ~18 ns. There is no clear transition in other results recorded at lower OPO pump-pulse energies (e.g., with $R_p = 2.5$ or $R_p = 2.0$).

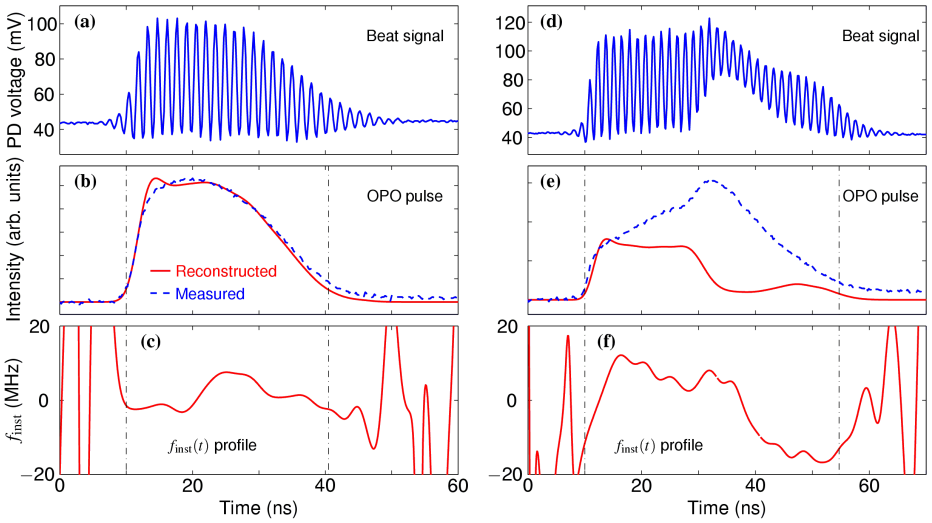

Fig. 4. OPO beat waveforms (a, d), intensity profiles (b, e), and instantaneous-frequency chirp profiles (c, f) for signal output from the long-pulse PPKTP OPO with low phase mismatch. Traces (a-c) correspond to SLM operation with lower OPO pump energy ($R_p = 1.55$) than in traces (d-f), where $R_p = 3.5$ and partial seeding sets in halfway through the OPO pulse. In traces (c) and (f), vertical dashed lines mark the 10%-intensity limits for the f_{inst} profile.

More pronounced partial seeding effects are observed in the context of Fig. 5, where $\lambda_s = 841.78$ nm (as in Fig. 4) but T_{PPKTP} is re-set at 125.1°C, giving $\lambda_{free} = 841.94$ nm and $(\lambda_s - \lambda_{free}) = -0.16$ nm (i.e., a relatively large phase mismatch). The corresponding frequency chirp measured with $R_p < 2.5$ in this set of experiments is –46 ± 3 MHz, reasonably close to the value of –58 ± 6 MHz predicted on the basis of Fig. 5 of ref. 1. The results for high pump-pulse energy (47 μJ, corresponding to $R_p = 3.5$) are presented in the static version of Fig. 5. The build-up of multimode operation now has a transition point ~12 ns after the start of the

#5338 - $15.00 US Received 20 September 2004; revised 3 November 2004; accepted 4 November 2004

OPO pulse (~6 ns earlier in the pulse than in Fig. 4, where the phase mismatch was smaller). For a dynamic view of the transient evolution of such partial seeding, click here; this reveals five sets of temporal profiles as the OPO pump-pulse energy is increased in successive steps from 21 μJ (R_p = 1.55), to 27 μJ (R_p = 2.0), to 34 μJ (R_p = 2.5), to 40 μJ (R_p = 3.0), and finally back to 47 μJ (R_p = 3.5). There are clear contrasts between the measured (dashed) and reconstructed (solid) OPO signal-pulse amplitude profiles from R_p = 2.5 upwards; the onset of partial seeding is seen to occur at a lower pump-pulse energy when $|\lambda_s - \lambda_{free}|$ and hence the phase mismatch is large (as in Fig. 5) compared with when it is small (as in Fig. 4).

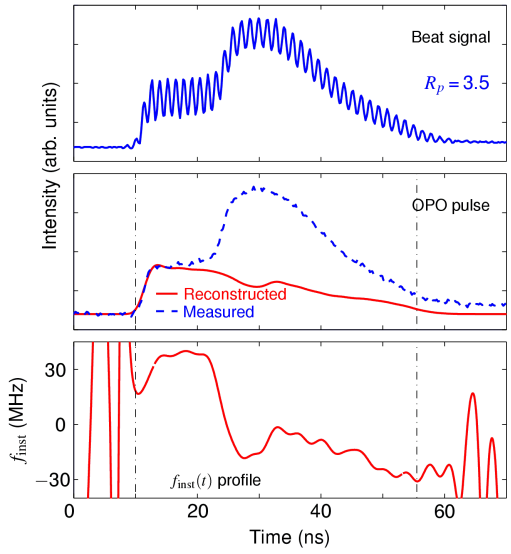

Fig. 5. Temporal waveforms with format as in Figs 4(a–c) or 4(d–f) for signal output from the long-pulse PPKTP OPO system with large phase mismatch and high OPO pump-pulse energy (R_p = 3.5). This results in partial seeding and multimode operation at a transition point earlier in the OPO pulse than in Fig. 4(d–f) (where R_p = 3.5 also but the phase mismatch and resulting frequency chirp are smaller), which is a more severe breakdown of SLM operation. (494 KB movie of a five-frame dynamic sequence of temporal profiles as pump energy is increased.)

4. Concluding discussion

Our investigation of the onset of multimode operation defines the pump-pulse energy below which reliable SLM, low-chirp operation is sustainable in an injection-seeded PPKTP OPO. The OH-based FT-analysis technique [1–3] yields unprecedented dynamical insight into the transition from SLM to multimode operation of a pulsed OPO. This depends on measuring the instantaneous frequency $f_{inst}(t)$ for the narrowband component of the OPO signal output radiation throughout the duration of the pulse, by beating the pulse against AOM-shifted cw seed radiation. Such OH-based measurements are able not only to monitor and control frequency chirp in narrowband pulses [1–3], but also to determine the pump-pulse energy threshold at which SLM OPO operation becomes unsustainable for the full duration of the pulse. For a TDL-seeded PPKTP OPO, with small $|\lambda_s - \lambda_{free}|$ to minimize phase mismatch and associated frequency chirp at a signal wavelength of ~840 nm, SLM operation is realized with 532-nm pump-pulse energies up to ~2.5 times the free-running (unseeded) OPO threshold (i.e., $R_p \leq 2.5$). This defines an upper limit to pump-pulse energy for SLM operation of the oscillator stage of higher-power OPO/OPA systems that are required for high-performance narrowband spectroscopic applications. Work on such higher-power systems is in progress.

Acknowledgments

We acknowledge financial support from the Australian Research Council.

#5338 - $15.00 US Received 20 September 2004; revised 3 November 2004; accepted 4 November 2004